FINITE ELEMENT MODELLING OF ULTRA-THIN CONTINUOUSLY REINFORCED CONCRETE PAVEMENT

P SMIT and E KEARSLEY

University of Pretoria, Private bag X20, Hatfield, 0028, South Africa
Tel: 012 362 5218, E-mail: phia.smit@up.ac.za

ABSTRACT

Ultra-Thin Continuously Reinforced Concrete Pavement (UTCRCP) is an innovative pavement type that typically consists of a 50 mm high strength steel fibre reinforced concrete layer overlaying existing or new pavement structures. The reduced thickness and high modulus of elasticity of the concrete layer makes it necessary to compare the response of UTCRCP to both conventional asphalt and concrete pavements. In this paper, the finite element method is used to investigate the effect of load configuration, concrete layer thickness and layer interaction on the response of road pavements.

1. INTRODUCTION & BACKGROUND

Road pavement design is a process intended to find the most economical combination of layer thickness and material types for pavements, considering the properties of the soil foundation as well as the environment and traffic loading during the service life of the road (Werkmeister *et al.*, 2004). The Mechanistic-Empirical Pavement Design (MEPD) approach incorporates the principles of engineering mechanics to predict the critical stresses and strains that a road pavement may experience (SANRAL, 2013).

The distinguishing feature of Ultra-thin Continuously Reinforced Concrete Pavement (UTCRCP) is that its overlay consists of a 50 mm, heavily reinforced, high strength continuously cast concrete slab (Kannemeyer *et al.*, 2007). The compressive strength of the concrete typically exceeds 100 MPa and approximately 80 kg/m^3 hooked-ended steel fibre is included in the mix design. Steel bar mesh, with an aperture of 50 mm and diameter of 5.6 mm, is placed mid-depth in the 50 mm overlay. Polypropylene fibres (2 kg/m^3) are included to control shrinkage cracking. The concrete layer is intended to be designed and constructed as part of new pavements (where it acts as the primary structural layer) or to be placed on existing pavements as rehabilitation. The high strength and high steel content allow, not only reduced concrete layer thickness, but also results in superior post-crack load carrying capacity of the concrete (Briggs *et al.*, 2016).

Concrete pavements are usually considered to be rigid pavement and modelled numerically by simplifying the substructure (all layers underneath the concrete layer) to a series of springs with a spring stiffness (or modulus of subgrade reaction). Although UTCRCP is a concrete pavement, the severely reduced thickness has led to a proposal that it should be analysed and designed as an asphalt (or flexible) pavement where permanent deformation in the substructure is also considered as a failure mechanism (Smit & Kearsley, 2018).

Advances in technology have made computing power more affordable and allows civil engineering systems to be modelled with more complexity. The finite element modelling of road pavement systems has advanced from assuming axisymmetry with static loading and linear-elastic material models to three-dimensional multi-layered assemblies with dynamic loading and complex material models (Cho *et al.*, 1996; Kannemeyer *et al.*, 2007).

The overall purpose of this research was to investigate the response of UTCRCP to loading. In this paper, three-dimensional finite element modelling was used to investigate the effect of:

- load configuration on road pavements with thin bound layers by considering single wheel and axle loading,
- relative stiffness of pavement layers by varying concrete bound layer thickness and base E-value using response surface methodology,
- layer interaction by varying the concrete bound layer – base interaction properties, and
- boundary conditions in terms of model depth.

A three-layer road pavement system consisting of a bound layer, base and subgrade was modelled. In this paper, a bound layer refers to a pavement layer that consists of a material such as asphalt or concrete. These materials are composed of aggregate which is bound together with a chemical substance. They have tensile strength and bend under loading (SANRAL, 2013). All materials were modelled using linear-elasticity. A static load was applied using a pressure over a circular area. The shape of the loaded area was not varied.

2. FINITE ELEMENT MODELLING

The general-use finite element program ABAQUS (Dassault Systemes Simulia Corp, 2016) was used. A three-dimensional finite element model was assembled. It was opted to replicate the geometry and mesh of a model used by Kim (2007) who determined the domain size of a finite element model that would be minimally affected by boundary conditions. The model load configuration was single wheel loading. This model was altered to investigate various aspects as mentioned in the purpose statement.

The horizontal and vertical dimensions of the road pavement model was given in terms of multiples of the radius (R) of the circular area over which the load was applied. The horizontal dimension was 20R and the vertical dimension was 140R. Quarter symmetry was used. The axis of symmetry in the longitudinal and transverse direction were taken at the centreline of the loaded area in the respective directions. The element type was three-dimensional quadratic hexahedron elements with reduced integration (C3D20R). The mesh fineness reduced with distance from load location. The circular load area had radius of 152.4 mm and a pressure of 550 kPa was applied to this area. This represented a 40 kN load, similar to that which would be carried by one side of a standard 80kN axle. The boundary conditions were set to restrict movement perpendicular to the boundary surface.

The pavement was modelled as a three-layer system that consisted of a bound layer, base and subgrade. The layer materials were modelled using a linear-elastic constitutive relationship. In the first part of the study, the effect of load configuration was investigated by modelling both single wheel and axle loading with either an asphalt bound layer or a concrete bound layer. The two materials considered were normal stiffness asphalt and high strength steel fibre reinforced concrete (Kearsley *et al.*, 2014; Kim, 2007; SANRAL,

2013) The layers, their thicknesses and material properties are shown in Table 1. Note that the bound layer thickness was initially set at 76 mm to match the thickness used by Kim (2007).

Table 1: Layer thickness and material properties

Layer		Thickness (mm)	E-value (MPa)	Poisson's ratio
Bound Layer (BL)	Asphalt	76	2 759	0.35
	Concrete		40 000	0.17
Base		305	207	0.4
Subgrade		140R-(BL+Base)	41	0.45

Axle loading was modelled by altering the single wheel loading model of Kim (2007). Once again quarter symmetry was used. The axis of symmetry in the longitudinal direction was taken at the centreline of an axle with a length of 1.98 m. The axis of symmetry in the transverse direction was taken along the centreline of the wheel and axle length. Instead of modelling only a quarter of the load area, half or the load area was modelled. A pressure of 550 kPa was applied. The model depth, layer thicknesses and material properties remained constant.

Figure 1 shows the geometry and mesh of the respective models. Figure 1.a shows the domain of the single wheel model as determined by (Kim, 2007). The total depth of the model was 21.336 m. Figure 1.b shows a plan and isometric view of the single wheel model. The model had a plan area of 3.048 x 3.048 m and the mesh fineness reduced from the load location. Figure 1.c shows a plan and isometric view of the axle load model. The figure shows half the circular area on which the pressure was applied and the longitudinal axis of symmetry that moved 0.99 m to the centreline of a 1.98 m axle. The plan area of the axle model was 3.048 x 4.047 m.

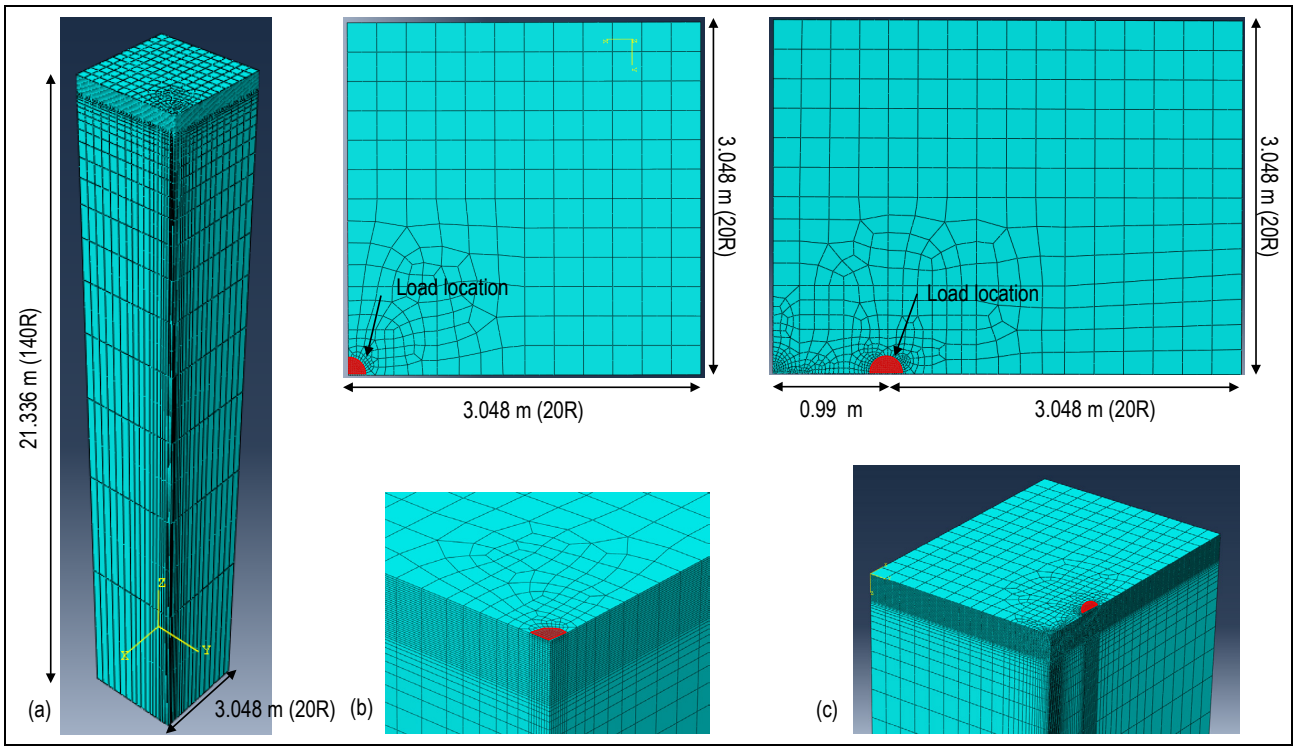

Figure 1: Geometry and mesh of a) complete model domain, b) single wheel and c) axle load configuration

In the second part of the study, Response Surface Methodology (RSM) was used to investigate the effect of relative stiffness of pavement layers on road pavement behaviour. RSM is a collection of mathematical and statistical tools used to model a response of interest which is influenced by several variables (Montgomery, 2001). Concrete bound layer thickness and base E-value were varied in this study. The three-layer road pavement model (bound layer, base and subgrade) was used along with the axle load configuration. The thickness of the base (305 mm) and the depth of the subgrade (21.155 m) remained constant, while only the concrete layer thickness and the E-value of the base were varied.

In RSM, a variety of response surface designs can be used to determine the values of the independent variables required for a given response surface model. In this study Central Composite Design (CCD) was used. CDD is an amended version of factorial design, and has axial and centre points. Figure 2 shows the factorial, axial and centre points used in CCD for a two-factor design. It also gives the coded variable level combinations ((0,0), (-1,1), (+1, -1)). The points situated on the corners of the square are the factorial points, the axial points are a distance “α” away from the centre point in the positive and negative x and y direction. The centre point is at the intersection of the x and y axes. The prediction quality of a response surface design is improved when it is rotatable. An α-value of 1.414 makes a two-factor CCD rotatable.

CCD makes it possible to efficiently develop first- and second-order response surface models (Montgomery, 2001). In the case of a two-factor CCD, only nine independent variable sets have to be tested (or modelled) to explore the region of interest. In the case of a traditional factorial design, combinations of equally spaced levels of the independent variables are used to explore a region of interest. If higher-order response surface models are to be fit to the data, the combinations of independent variables have to be more densely spaced.

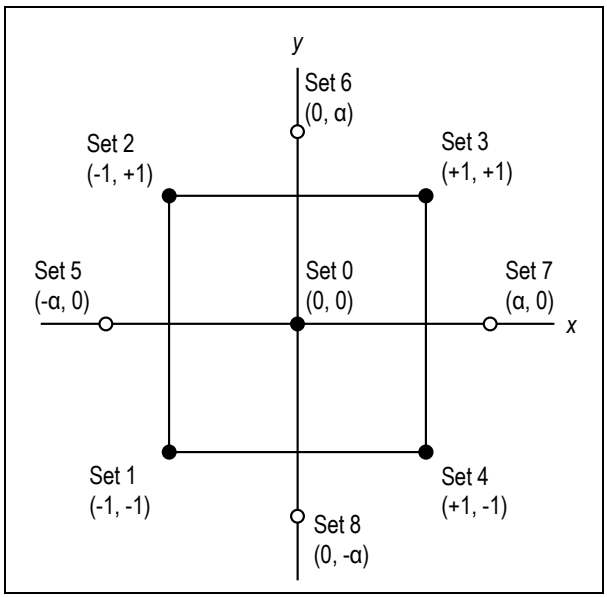

Figure 2: Central Composite Design (Montgomery, 2001)

The combinations of concrete layer thickness and base E-value analysed can be viewed in Table 2. The base E-value was varied from 40 MPa to 700 MPa and the concrete layer thickness was varied from 30 mm to 346 mm. The base E-value range was selected from *Pavement design* (SANRAL, 2013) as the minimum and maximum values for granular materials for the Pavement Number Design Method. The concrete layer thickness range

was selected to smaller than the thickness of UTCRCP (50 mm) and greater than the typical conventional concrete thickness (300 mm).

Table 2: Central composite design variable value combinations

	Coded independent variable level		Independent variables	
Multivariable combination	x	y	Thickness (mm)	MoE (MPa)
Set 0	0	0	188	370
Set 1	-1	-1	76	137
Set 2	-1	1	76	603
Set 3	1	1	300	603
Set 4	1	-1	300	137
Set 5	-1.414	0	30	370
Set 6	0	1.414	188	700
Set 7	1.414	0	346	370
Set 8	0	-1.414	188	40

In the third part of the study, the effect of the concrete bound layer – base interaction was investigated. A contact property was assigned for the concrete layer – base interaction. For the purposes of this study the contact property consisted of the tangential and normal behaviour between the two layers. The three-layer road pavement model (bound layer, base and subgrade) was used along with the axle load configuration. For the normal behaviour “Hard” contact was used and separation after contact was allowed. “Hard” contact minimizes penetration of the slave nodes (base) into the master surface (concrete bound layer) and does not allow the transfer of tensile stress across the interface (Dassault Systemes Simulia Corp, 2014). Any pressure can be transmitted between the surfaces when they are in contact. The surfaces separate when the contact pressure reduces to zero and separated surfaces come into contact when the clearance between them reduces to zero.

For the tangential behaviour a penalty friction formulation was used. The directionality was isotropic, and a friction coefficient was assigned. The Coulomb friction model is used. It defines the critical shear stress at which sliding between the surfaces start as a fraction of the contact pressure. The fraction is known as the friction coefficient and the values considered in the study were 0.35 and 0.6, which were the minimum value for friction between concrete and fine sand and the maximum value for friction between concrete and coarse sand (Department of the Navy, 1982). Frictionless interaction was also modelled.

The focus of this research is on UTCRCP which has a 50 mm concrete layer and not a 76 mm concrete layer (as used in the first part of the study). In the fourth part of the study, the thickness of the concrete layer was changed to 50 mm. The effect of model depth was investigated by decreasing the depth from 21.366 m to 4.038 m. The three-layer road pavement model (bound layer, base and subgrade) was used along with the axle load configuration. In this part interaction was not modelled and only the subgrade depth was decreased.

3. RESPONSE OF ROAD PAVEMENT MODELS

Critical parameters for road pavements suggested by Kim (2007) were used to evaluate the effect of the various aspects mentioned. These critical parameters were taken along the centreline of the circular load area and were;

- the vertical displacement at the pavement surface,
- the horizontal tensile stress in the bound layer, and

- the vertical compressive stress and strain in the subgrade.

Figure 3 shows the location of the critical parameters in the single wheel model. The values extrapolated to the nodes at the respective locations were used. The Response Surface Methodology contour plots (or response surfaces) were determined for the same critical parameters. Additionally, the deflected shape of the road pavement surface and contour plots of the vertical and horizontal displacement were considered.

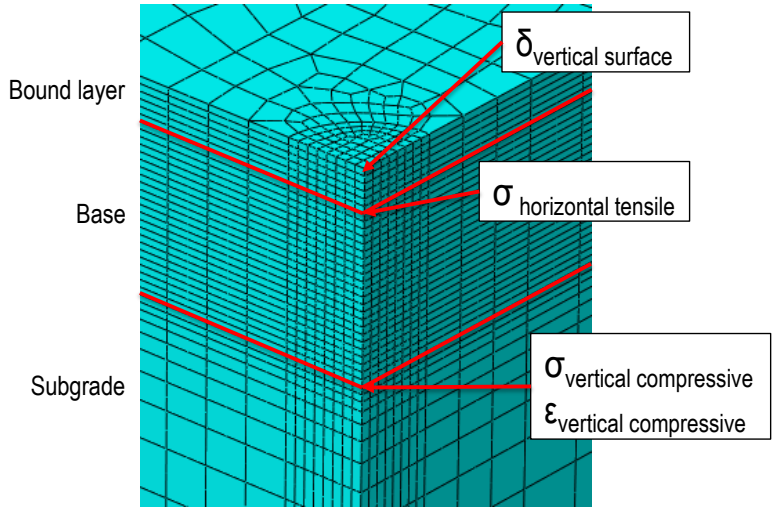

Figure 3: Critical parameters and their locations

3.1 The effect of load configuration on road pavements with thin bound layers

The critical parameters of both asphalt and concrete bound layer pavements with single wheel and axle load configuration are summarised in Table 3. The vertical displacement of the asphalt model was higher than that of the concrete model. The horizontal tensile stress at the bottom of asphalt layer was lower than the concrete layer, but the vertical compressive stress and strain in the subgrade was higher. This behaviour illustrates the structural dominance of the concrete bound layer which has an E-value of 40 000 MPa instead of 2 597 MPa for asphalt. The high E-value induced wider load spreading in the concrete layer, which reduced stress in the base and subgrade.

Table 3: Critical parameters for asphalt and concrete bound layer pavements

	Asphalt			Concrete		
Critical parameter	Single wheel	Axle	Difference[#] (%)	Single wheel	Axle	Difference[#] (%)
$\delta_{vertical\ surface}$ (mm)	-0.913	-1.011	-10.75	-0.590	-0.692	-17.32
$\sigma_{horisontal\ tensile}$ (kPa)	1 364	1 362	0.092	4 747	4 637	2.314
$\sigma_{vertical\ compressive}$ (kPa)	-41.7	-41.9	-0.508	-21.9	-22.3	-1.791
$\varepsilon_{vertical\ compressive}$ (µm/m)	-974	-965	0.879	-473	-466	1.395
[#]Difference (%) = ((Single wheel$_{value}$-Axle$_{value}$)/Single wheel$_{value}$)*100						

Changing the load configuration from single wheel to axle loading affected both bound layer models. The vertical displacement increased. This is because;

- an axle with two wheels is applied to the axle model resulting in 80 kN load applied instead of only 40 kN as for the single wheel model, and
- the zone of influence, due to the load applied to each wheel, increases with depth and at a certain depth the zones overlap in the axle model, doubling the displacement in those regions.

The increase in vertical displacement, due to change in load configuration, was more for the concrete model than the asphalt model. This can also be explained by the wider load spreading ability of the concrete, where the zone of influence of the respective wheels start overlapping at a shallower depth. Although the effect of the load configuration change was minimal for the other critical parameters, the concrete model was affected more significantly.

The horizontal tensile stress experienced at the bottom of the 76 mm concrete layer for both models was in the range of 4 700 kPa. The horizontal tensile stress experienced at the top of the concrete layer along the axle centreline was 702 kPa. The modulus of rupture of normal strength concrete (30 MPa compressive strength) about 4 MPa (Domone & Illston, 2010). Considering the S-N curve for normal concrete in Huang (1993), a 76 mm layer of normal strength concrete would fail after a minimal amount of load repetitions. The modulus of rupture of high strength steel fibre reinforced concrete (91.7 MPa compressive strength) is approximately 11.7 MPa (Kearsley *et al.*, 2014). The high strength reduces the stress/strength ratio to less than 0.5 and the steel fibre content give the material post-crack load carrying strength. UTCRCP has been shown to have a minimum life of 25 million standard axle loads (Kannemeyer *et al.*, 2007).

Figure 4 shows normalized deflection plots of the surface of the four models considered. The deflection plots were each normalized with respect to their own maximum deflection to aid comparison. The region from the axle centreline to 1 m to the right of the wheel centreline is shown. The deflection plots of the single wheel models are reflected around their axis of symmetry (wheel centreline) for comparative purposes.

The normalized deflection of single and axle loading for both bound layer types compared well from the wheel centreline to the right. The deflection from the wheel centreline to the axle centreline did not compare well. Axle loading resulted in hogging type deflection along the axle centreline where tensile stresses would be induced at the top of the bound layer (concrete or asphalt). The normalized deflection bowl was wider for the concrete model, indicating improved load spreading where a larger fraction of the total deflection is spread over a greater area.

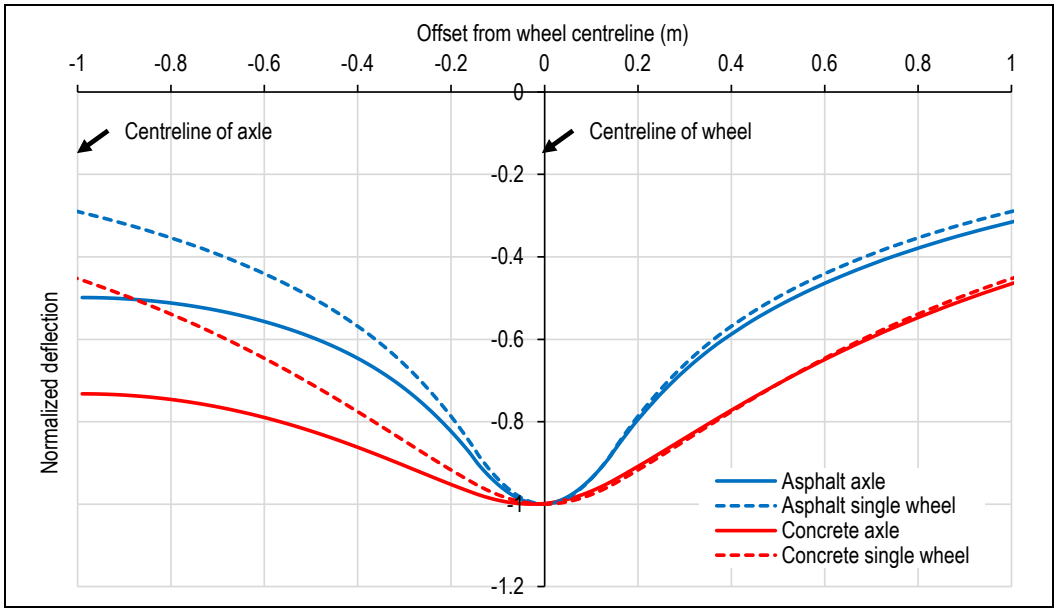

Figure 4: Normalized deflection of respective bound layer – load configuration combinations

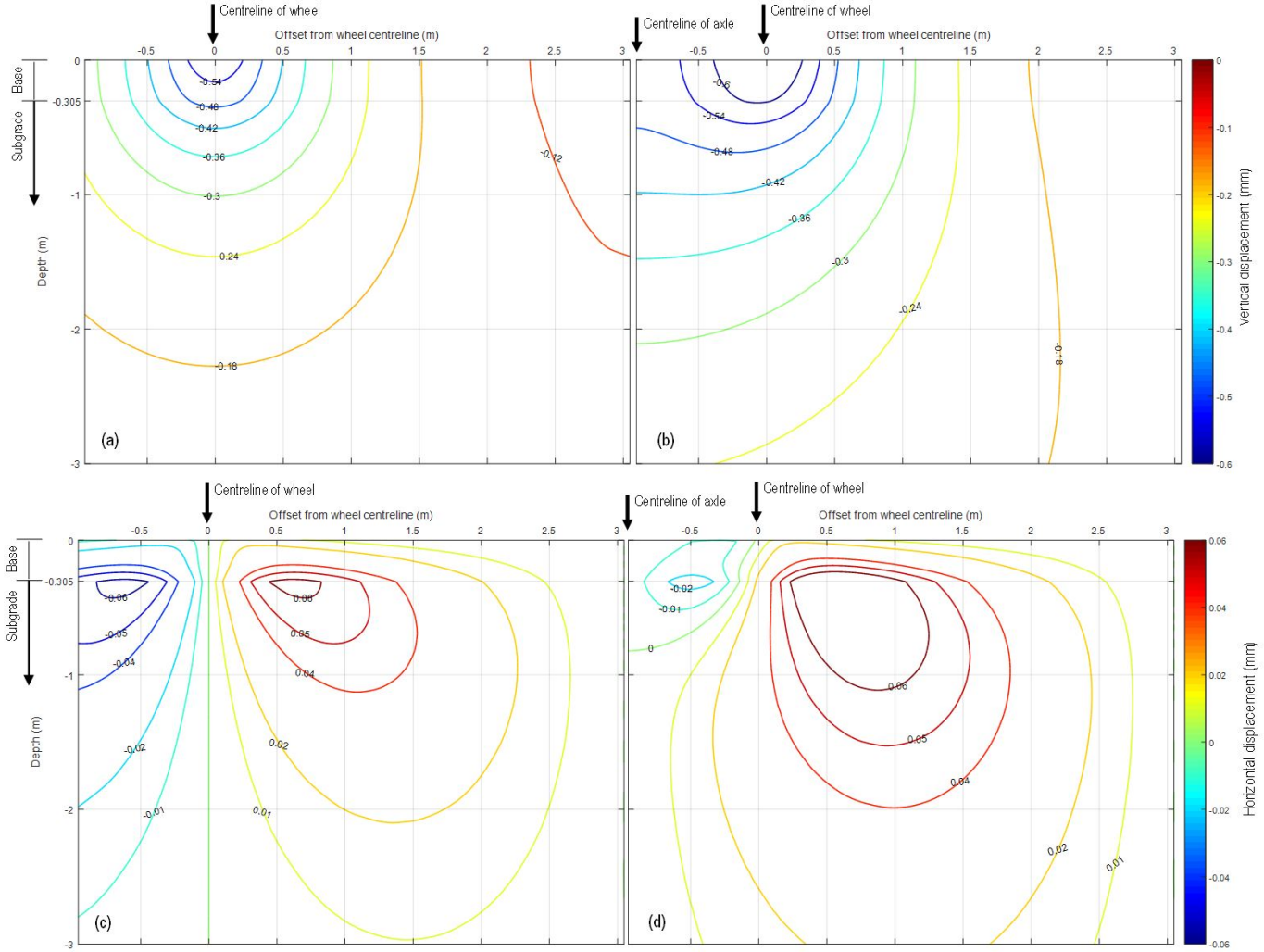

Figure 5: Contour plots of a) single wheel vertical -, b) axle vertical -, c) single wheel horizontal - and d) axle horizontal displacement

Figure 5 shows the displacement contour plots of the four models. The full width of the model and a depth of 3 m was included in the contour plot. The displacement of the bound layer was excluded. Similar to the deflection plot of the single wheel models, the displacement contours were reflected about their axis of symmetry (the centreline of the wheel) for comparative purposes. Figure 5.a shows the symmetrical vertical displacement of the single wheel model. In Figure 5.b, it can be seen that the horizontal offset of the maximum vertical displacement, moved from the centreline of the wheel toward the centreline of the axle, with depth. This was due to an increase in the overlap of the zones of influence of the two wheel loads with depth.

The horizontal displacement was order of magnitude smaller than the vertical displacement for both load configurations. Figure 5.c shows the symmetrical horizontal displacement of the single wheel model. Figure 5.d shows the horizontal displacement of the axle load model. The figure shows that the section of horizontal displacement that was moving to the right of the model reached past the wheel centreline toward the axle centreline with depth. A small, shallow section (depth of 1 m) located between the wheel centreline and axle centreline displaced toward the axle centreline. Modelling the substructure using finite elements allowed its response to be investigated in more detail. The locations where permanent deformation would manifest in road pavements loaded using a single wheel would be different than in road pavements loaded using an axle.

3.2 The effect of relative stiffness of the concrete bound layer thickness and base E-value by using Response Surface Methodology

Figure 6 shows the contour plots of response surfaces determined through regression analysis of the CCD data points. The model equations of each critical parameter had to be transformed using a Power transformation. Although the coefficient of determination of the model equations were high (>99%) other diagnostic tools indicated that they were not significant (Montgomery, 2001). Nonetheless, some observations can be made regarding the effect of relative stiffness. The response of the pavement was more dependent on the thickness of the concrete layer than the base E-value. At smaller thicknesses the response becomes a little more dependent on the base E-value. This change in dependence, although small, is the largest for the horizontal tensile stress at the bottom of the concrete layer.

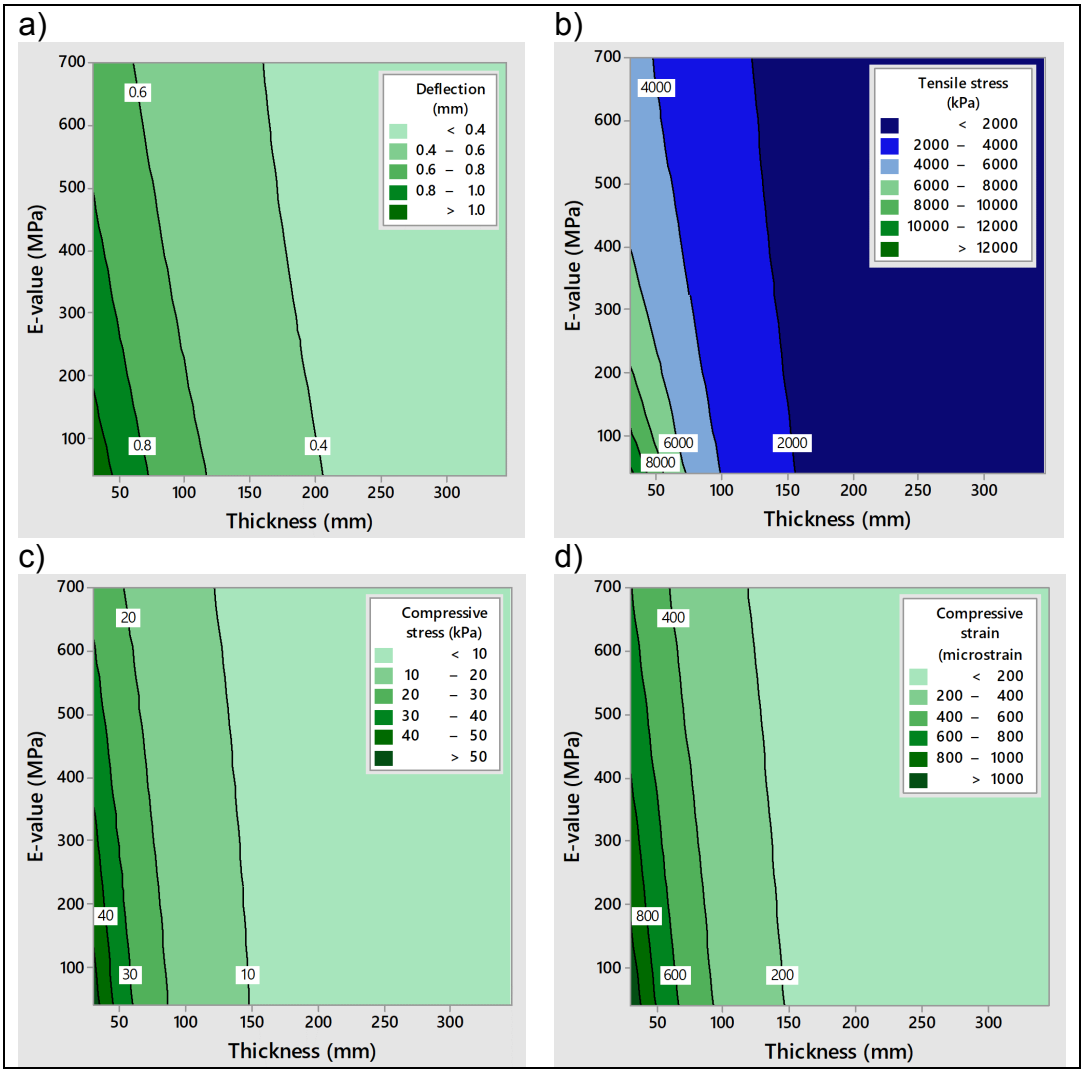

Figure 6: Response surfaces of critical parameters

The dominant effect of the concrete layer thickness is related to the concept of flexural stiffness of rectangular sections where the effect of thickness is raised to the power of three. In this case a cube response surface model would have been more suitable and the use of an alternative response surface design (to CCD) would have been beneficial.

Figure 7 below shows the deflection plots of the factorial and centre points of the response surface design used. It shows that varying the base E-value from 137 MPa to 603 MPa had very little effect on the deflected shape and magnitude of the models with a 300 mm thick concrete layer (Set 3 and 4). This supports the assumption that the response of rigid pavements is not influenced significantly by the substructure and that it can be simplified to a series of springs. The maximum deflection in these models was at the axle centreline. The shape of these deflection plots was similar to single curvature.

The shape of the deflection plot of the models with a 76 mm thick concrete layer (Set 1 and 2) was not similar to single curvature. The maximum deflection occurred under the wheel centreline and there was hogging type deflection at the axle centreline. The vertical and horizontal displacement of the substructure would be similar to that in Figure 5.b and Figure 5.d. This supports the proposal that UTCRCP should be considered as a flexible pavement where rutting is a failure mechanism and that the effect of permanent deformation should be investigated using advanced material models. The deflection of Set 0 was similar to models with the thick concrete layer, although the maximum deflection was not in the axle centreline, but under the loaded area.

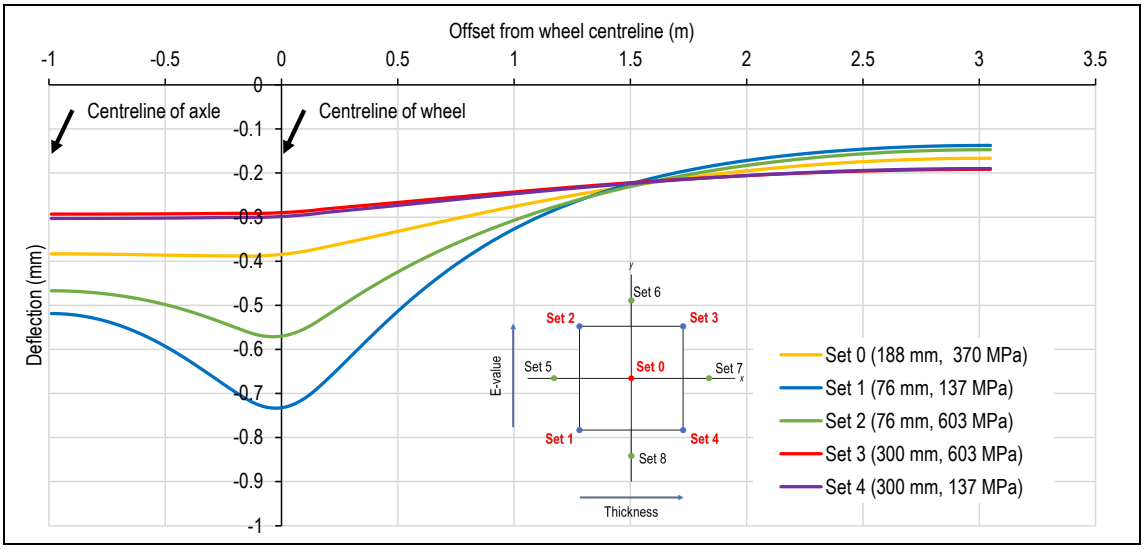

Figure 7: Deflection plots of factorial and centre sets

3.3 The effect of concrete bound layer – base interaction and model depth

The effect of interaction was determined by allowing normal and tangential movement of the concrete bound layer with respect of the base layer. The only normal behaviour modelled was “Hard” contact allowing separation. The coefficient of friction was varied for the tangential behaviour. The critical parameters in Table 4 show the effect of including interaction. “Perfect bond” refers to the model discussed in Section 3, where interaction was ignored, and the layers could not move with respect to each other. Allowing the concrete layer to detach from the base influenced the critical parameters more than subsequently varying the coefficient of friction. Increasing the coefficient of friction decreased the critical parameters minimally. The horizontal tensile stress in the concrete bound layer increased by approximately 13%, which supports previous research that noted that debonding of the concrete layer affects the performance of UTCRCP significantly (Kannemeyer et al, 2007).

Table 4: Effect of interaction on critical parameters

Critical parameter	Interaction			
	Perfect bond	Friction-less	μ=0.35	μ=0.6
$\delta_{vertical\ surface}$ (mm)	-0.692	-0.778	-0.777	-0.774
$\sigma_{horisontal\ tensile}$ (kPa)	4 637	5 276	5 251	5 235
$\sigma_{vertical\ compressive}$ (kPa)	-22.3	-29.1	-28.9	-28.7
$\varepsilon_{vertical\ compressive}$ (μm/m)	-466	-520	-517	-514

The concrete layer thickness was changed to 50 mm, the entire model was then reduced to a depth of 4.038 m. The critical parameters in Table 5 increased when the concrete bound layer thickness was reduced. Decreasing the model depth (labelled as “50 mm reduced depth”) resulted in reduced deflection, but the other critical parameters were not affected significantly.

Table 5: Effect of model alteration on critical parameters

Critical parameter	76 mm	50 mm	50 mm reduced depth
$\delta_{vertical\ surface}$ (mm)	-0.692	-0.862	-0.706
$\sigma_{horisontal\ tensile}$ (kPa)	4 637	6 914	6 911
$\sigma_{vertical\ compressive}$ (kPa)	-22.3	-33.8	-33.9
$\varepsilon_{vertical\ compressive}$ (μm/m)	-466	-749	-811

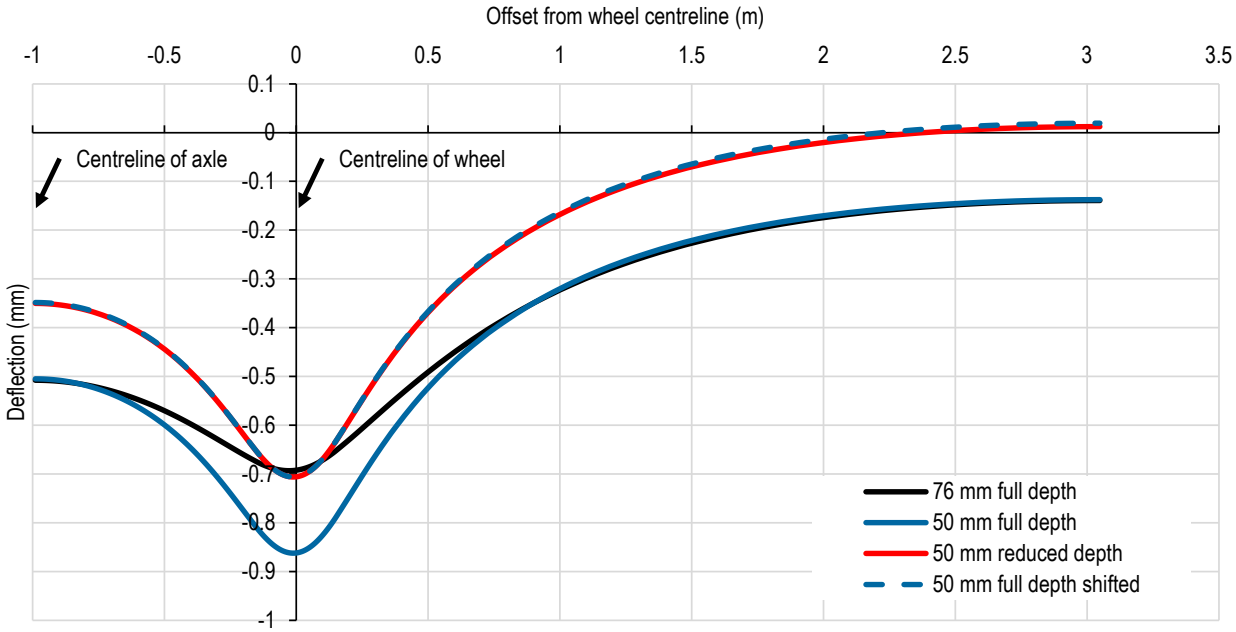

Figure 8: Deflection plots of model alterations

Figure 8 shows the deflection plots for the different models. Reducing the concrete bound layer thickness results in greater deflection around the load location. From an offset of 0.5 m from the wheel centreline, the deflection of the 76 mm and 50 mm models start converging again. Reducing the depth of the model reduced the deflection. The deflection plot of the full depth 50 mm model was “shifted” upward by the distance between its maximum deflection and the maximum deflection of the reduced depth model. The deflected shape of the full depth 50 mm model and the reduced depth 50 mm model was approximately the same. The reduced depth model deflected upward from approximately 2.25 m from the load location toward the rights. This indicates that the free edges of thin

concrete pavements, constructed on shallow layerworks with horizontal rock faces close to the surface, may deflect upwards under load.

4. CONCLUSION AND RECOMMENDATIONS

Based on the results of the three-dimensional finite element models of road pavements it could be concluded that both pavements with thin asphalt and concrete bound layers would benefit from being modelled with complex load configurations. Although critical parameters were not significantly affected the overall response of the axle load models were significantly different than the single wheel models. The vertical and horizontal displacement in the substructure for the single wheel and axle loading was also significantly different.

Varying the relative stiffness led to the conclusion that the concrete thickness had a dominant effect on the critical parameters. The deflection plots of selected thickness – E-value combinations showed that the deflected shape changed as the concrete layer became thinner. Thick concrete layer had single curvature with the maximum deflection occurring along the axle centreline. The thin concrete layers had maximum deflection along its wheel centreline with hogging along the axle centreline.

Allowing the concrete layer to detach from its supporting layer has a greater influence on the critical parameters than varying the friction between the layers. Including interaction increased the critical parameters. Reducing the depth of the road pavement model had little effect on the critical parameters, although it resulted in the upward movement of the model free-end at the right.

From the results presented in this paper it is recommended that the response of UTCRCP should be further investigated to consider the stress and strain induced in the substructure using linear-elastic material properties. Furthermore, the effect of using complex material models for the granular materials should be determined. Including the stress dependency, low tensile strength and permanent deformation of granular material may lead to significant stress redistribution in pavement systems. It is also recommended that the effect of pavement boundary conditions should be investigated using both linear-elastic and complex material models.

5. REFERENCES

Briggs, MA, Valsangkar, AJ & Thompson, A. 2016. Behaviour of fibre-reinforced concrete beams on grade. *Int. J. Phys. Model. Geotech.* 16(4), pp 152-159.

Cho, Y-H, McCullough, BF & Weissmann, J. 1996. Considerations on Finite-Element Method Application in Pavement. *Transp. Res. Rec.* 1539, pp 96-101.

Dassault Systemes Simulia Corp. 2014. *ABAQUS Documentation*. Providence, RI, USA.

Dassault Systemes Simulia Corp. 2016. *ABAQUS*. Johnston, RI, USA.

Department of the Navy. 1982. *Foundations and Earth Structures.* Alexandria, VA, USA.

Domone, P & Illston, J. 2010. *Construction Materials,* 4th ed., Oxon: Spon Press

Huang, YH. 1993. *Pavement Analysis and Design,* 2nd ed., New Jersey: Pearson Prentice Hall.

Kannemeyer, L, Perrie, BD, Strauss, PJ & Du Plessis, L. 2007. Ultra-Thin Continuously Reinforced Concrete Pavement research in South Africa., in: *Int. Conf. on Concrete Roads*, August 2007. Midrand, South Africa: Cement & Concrete Insitute, pp. 97-124.

Kearsley, EP, Vd Steyn, WJ vdM, & Jacobsz, SW. 2014. Centrifuge modelling of Ultra Thin Continuously Reinforced Concrete Pavements (UTCRCP). In *Physical Modelling in Geotechnics; Proc. of the 8th Int. Conf.*, 14-17 January 2014. Perth, Australia: Taylor & Francis Group, pp. 1101-1106.

Kim, M. 2007. Three-dimensional finite element analysis of flexible pavements considering nonlinear pavement foundation behaviour. University of Illinois at Urbana-Champaign.

Montgomery, DC. 2001. *Design and analysis of experiments*. 5th ed. New York: John Wiley and Sons.

SANRAL, 2013. Pavement Design, in: South African Pavement Engineering Manual. SANRAL Ltd: South Africa.

Smit, MS & Kearsley, EP. 2018. Investigating the response of Ultra-Thin Continuously Reinforced Concrete Pavements to initial loading., in: *13th International Symposium on Concrete Roads*. June 2018. Berlin, Germany: EUPave.

Werkmeister, S, Dawson, AR & Wellner, F. 2004. Pavement Design Model for Unbound Granular Materials. *J. Transp. Eng.* 130(5), pp 665-674.